

# Silver nanoparticles synthesis in water solution of maleic anhydride copolymers

D. DONESCU, R. SOMOGHI\*, V. PURCAR, S. SERBAN,  
M. GHIUREA, C. PETCU, C. RADOVICI, R. FIERASCU

*National Research & Development Institute for Chemistry and Petrochemistry ICECHIM, Polymer Department,  
Bucharest, Splaiul Independentei 202, Sector 6, Bucharest, Romania*

A variety of silver nanodispersions were synthesized in aqueous solutions of polyelectrolytes obtained from alternating copolymers of maleic anhydride with styrene sulfonide (StSO<sub>3</sub>, MA) and with vinyl acetate (VAc-MA). The smaller size of the aggregates depends on the concentration of the organic component and assure Ag<sup>0</sup> particle stability. Synthesized nanoparticles were observed by XRD and SEM analyses and evidenced the presence of face centered cubic structured nanocrystals, with a higher degree of structural order in solid phase for low polyelectrolyte concentrations. DLS analyzes show that Ag<sup>0</sup> nanoparticles dimensions increases with the increase of the polyelectrolyte concentration. Using UV, fluorescence and X-ray spectra analysis we have explored the effects of Ag<sup>0</sup> nanoparticles presence.

(Received March 3, 2010; accepted June 16, 2010)

*Keywords:* Silver Particles, Copolymer, Nanodispersion, Polyelectrolyte, Hybrid

## 1. Introduction

Nanocomposites metal polymers have attracted great interest due to their diversity for advanced technologies (1). Nanodispersed silver has been used in order to obtain materials with antibacterial, photosensitive, catalytic properties. Ag<sup>0</sup> nanoparticles synthesis in presence of polar polymers depends on the concentration of macromolecular compounds and on the side groups presence able to form metal chelate [2- 4].

Polyelectrolytes tend to have strong interactions with metal due to the functional groups like: sulphate [5-8], carboxyl [9-17], amide [12,13], amine [5, 6, 8, thiol (19). These interactions between polyelectrolyte gels and metal [11 – 13, 20] are the reason why polyelectrolytes may be used as nanoreactors in forming stabilized silver nanoparticles.

It is well known the fact that in aqueous solutions polyelectrolyte conformation is strongly affected by the concentration (21). Based on this information, this study focuses on Ag<sup>0</sup> nanoparticles formation in polyelectrolyte solutions with different concentrations and structures. Alternating copolymers maleic anhydride (MA) with vinyl acetate (VAc) [22] and 4- styrene sulphonate (StSO<sub>3</sub>) dispersed in water with Na salts are used as polyelectrolytes. The mean diameters and the Zeta potential of the metallic nanoparticles are studied, function of polyelectrolytes and Ag concentrations.

Ag<sup>0</sup> dispersions obtained from the two polyelectrolytes were comparatively analyzed through UV. Optical plasmon resonance of the metallic particles interacted with polymers depend by the dielectric functions of the metal and polymers, by the interface

between particles and surrounding medium and by the particle size and shape distributions [23]. When the used polymer is known,  $\lambda_{\max}$  corresponding to the plasmon adsorption band depends on the Ag<sup>0</sup> particle dimensions and local environment [8-18].

Ag<sup>0</sup> concentration influence on the thermal stability was estimated by TGA and metallic particles, while sedimentation after water evaporation was studied through SEM.

## 2. Experimental

### 2.1 Materials

Vinyl acetate (VAc), commercial product and acetone (Chimopar) were purified through rectification. Maleic anhydride (MA) was purified through sublimation. Azoizobutyronitril (AIBN) (Riedel de Haen) was used after recrystallization from methanol. Copolymer styrene sulphonate – MA (Aldrich) were used without any purification. Silver azotize (AgNO<sub>3</sub>) (Fluka) and sodium borohydride (NaBH<sub>4</sub>) (Fluka) were used as such.

### 2.2 Methods

VAc-MA copolymer was obtained through alternating copolymerization in acetone as shown in [12].

Silver nanoparticles were synthesized in polyelectrolyte, solutions obtained through VAc-MA copolymer neutralization with NaOH until pH=7. This copolymer, as well as the other polyelectrolyte StSO<sub>3</sub>-MA copolymer (formula gave by the producer C<sub>12</sub>H<sub>10</sub>Na<sub>2</sub>O<sub>7</sub>S), were used as aqueous solutions of 10%, 1% and 0,1% gravimetric. The initial reaction mixture contained 60 g of

the mentioned solutions. Different quantities of  $\text{AgNO}_3$  dissolved in 10 cc water were added on this solution (Table 1). The whole mixture was heated at  $65^\circ\text{C}$  under stirring (350 rot/min.) and was maintained like that for 3 hours. After a night without stirring, a adequate quantity of  $\text{NaBH}_4$  diluted with 10cc  $\text{H}_2\text{O}$  (for example at 0.0584 g  $\text{AgNO}_3$  were used 0.052 g  $\text{NaBH}_4$ ) was poured in drops, while the whole mixture was stirred. In case of aqueous solutions without polyelectrolyte, this  $\text{NaBH}_4$  quantity assures total transformation of  $\text{AgNO}_3$  in  $\text{Ag}^0$ .

The particle dimensions distribution, the mean diameter and the Zeta potential were measured with an instrument Zetasizer Nano ZS, ZEN 3600 produced by Malvern International LTD.

UV spectra were done on a UV Nicolet 500 instrument.

IR spectra were measured on dried samples mixed with KBr with an FTIR-Tensor 30 BRUCKER instrument.

The thermogravimetric analyzes (TGA) were done with a Du Pont 2000 instrument at a heating rate of  $20^\circ\text{C}/\text{min}$ . in air.

SEM images of aqueous dispersions with a minimum concentration of polyelectrolyte were obtained with an FEI Quanta 200 instrument (Fig. 7). For higher concentrations of polyelectrolyte, samples were diluted and examined.

The instrument is the fluorescence spectrometer with energy dispersion PW 4025 MINIPAL, produced by PanAnalytical.

XR diffractograms were registered with an DRON 2,0 diffractometer using a  $\text{CuK}\alpha$  ( $\lambda=1.5418\text{\AA}$ ) radiation, filtered with Ni for the  $\text{K}\beta$  component elimination. To determine the crystals dimensions, the Scherrer equation has been used between the diffraction maxima half width corrected for the instrument width, and the mean size of the crystalites  $D\lambda K I = K\lambda/\beta\cos\theta$  where  $K=0.85$  – constant and  $\theta$  is the diffraction angle.

### 3. Results and discussion

First, we tried to establish that alternating copolymers VAc-MA and  $\text{StSO}_3$ -MA tend to form in water polyelectrolyte solutions. Viscosimetric method was used to measure the reduced viscosity and obtained values confirm the polyelectrolytes behavior (Fig. 1). An increase in viscosity ( $\eta_{sp}/c$ ) was observed at the same time with increasing the dilution (21) of the samples.

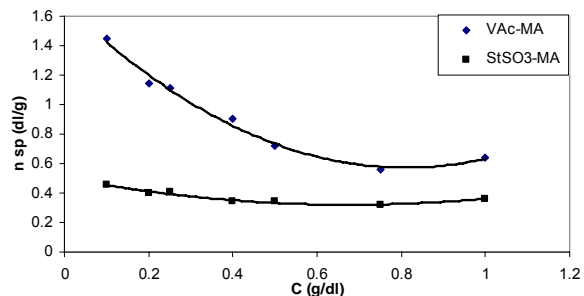


Fig.1. Specific viscosimetry function of the concentration of VAc-MA and  $\text{StSO}_3$ -MA copolymers

The synthesis conditions of various compounds are summarized in Table 1. It is noteworthy that 4-styrene sulphonate copolymers at higher concentrations may ensure  $\text{Ag}^0$  nanoparticles stabilization. The sulphonate group presence, comparing to two carboxylic groups, can give a higher stability for the synthesized particles (8, 24).

Table 1. The synthesis conditions of the  $\text{Ag}^0$  nanoparticles (for 80 g mixture).

Copolymer	$\text{AgNO}_3$ (g) / No. sample				
	0,0584	0,1168	0,1752	0,2336	0,584
Cop. (g) VAc-MA 6	3103	3119	3117	-	3106
0,6	3104	3120	3118	-	3107
0,06	3105	3121	3116	-	3108
Cop. (g) $\text{StSO}_3$ -MA 6	3138	3141	3136	3144	3153
0,6	3139	3142	3137	3145	3154
0,06	3140	3143	3135	3146	3155
-	3115				

If the transformation of  $\text{AgNO}_3$  in  $\text{Ag}^0$  is considered quantitative, the maximum quantity of stabilized metal, for VAc-MA copolymer (concentration 1%), is 0.123g Ag for 1g copolymer. For  $\text{StSO}_3$ -MA copolymer, when we increase the quantity of the metal to 0.618 g  $\text{Ag}^0$  for 1g copolymer, the synthesis takes place without precipitation.

The influence of polyelectrolyte concentration and the initial quantity of  $\text{AgNO}_3$  on  $\text{Ag}^0$  particle dimensions are presented in Fig. 2.

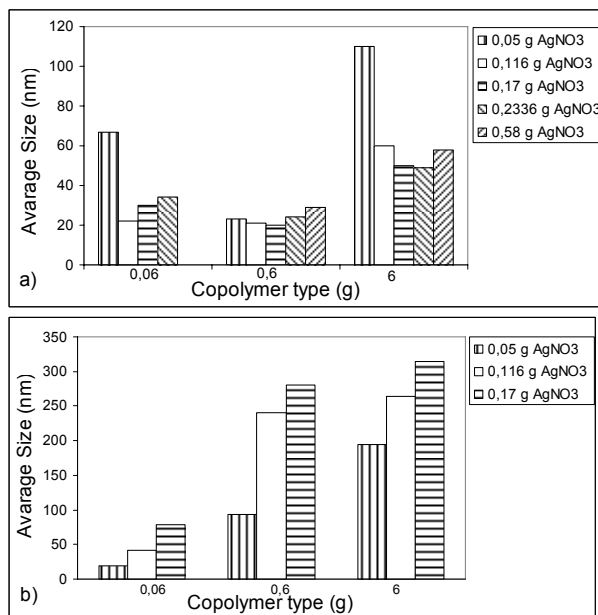


Fig. 2. Average size of  $\text{Ag}^0$  synthesized particles with  $\text{StSO}_3$ -MA (a) and VAc-MA (b) copolymers

The mean size of the particles for both polyelectrolytes increase with the increase of the polymer concentration. Diameters of  $\text{Ag}^0$  particles obtained on VAc-MA copolymer (Fig.2b) are higher than the diameters of the  $\text{Ag}^0$  particles obtained on the copolymer with sulphonic groups (Fig.2a), result which confirms the conclusions from Tab.1 regarding  $\text{StSO}_3$ -MA polyelectrolyte, which may offer a higher stabilization for the final particles.

Distribution curves of the particles dimensions are not monomodal (Fig. 3). There are two main generation of particles: one with small dimensions and the other of higher dimension, probably due to the small particles association. The percentage of the generation of small dimension is higher for  $\text{StSO}_3$ -MA copolymers, fact which may prove this particles higher stabilization (Fig. 3a). Also  $\text{StSO}_3$ -MA copolymers have a generation of high dimension particles but with smaller values than in VAc-MA copolymer case. These results are in concordance with the results previously published [24].

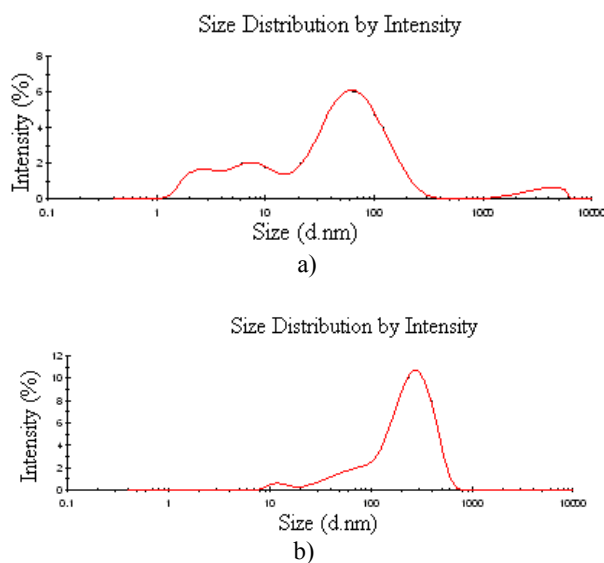


Fig. 3. Distributions curves of the average size particles for samples with 0.1168 g  $\text{AgNO}_3$  and a-0.6g  $\text{StSO}_3$ -MA/b-0.6g VAc-MA.

The diameter increases with the increase of the copolymers concentration. This increase can be explained by the macromolecules association [21], the template effect of the functional groups [20], as well as by the mechanism of the metal particles generation in the presence of polymer chains [3, 4, 25].

The study of  $\text{Ag}^0$  nanoparticles synthesis through  $\text{AgNO}_3$  reduction with  $\text{NaBH}_4$  in the presence of poly(N-isopropylamide) solutions distinguishes the polymer's role of nucleating, coupling and stabilizing agent (26). SEM images of the final metal particles evidence increased aggregate when the polymer concentrations increase. These analyses have similar results as the DLS analyses from Fig. 2.

Data from Fig. 2 and Table 1 reveals some unexpected results. At low concentrations of  $\text{AgNO}_3$ , the final

dispersion's stability decrease and the average diameter of the particles is higher for the  $\text{StSO}_3$ -MA hydrophilic copolymer (Fig.2a). These increased average diameters demonstrate a weak stabilization of the  $\text{Ag}^0$  particles obtained through  $\text{NaBH}_4$  reduction.

It is a well known fact that organic acids [27] and sodium dodecil sulphate [28] form silver salts in the presence of inorganic salts of this metal. Also is often mentioned the polyelectrolyte interactions which contains sulphonate [8] or carboxyl groups [10-17]. The two carboxyl groups from the structural unit of MA and the sulphate from the  $\text{StSO}_3\text{Na}$  can ensure the synthesis with silver salts, the aim of this study.

These Ag salts are less soluble in water, the initial transparent mixture turns to opaque after  $\text{AgNO}_3$  adding and induces the stabilization effect for the new metal particles [8,13-15]. The decrease of the  $\text{AgNO}_3$  concentration reduces the concentration of these stabilizers which leads to aggregation of the metallic particles. This aggregation effect leads to large particles forming (Fig. 2) and to destabilization of the initial dispersions at lower  $\text{AgNO}_3$  concentrations (Table 1). The action way of in situ stabilizers is similar to association method through hydrophobic demixing of the hydrophobic modified polyelectrolites [29]. The similarity is due to VAc-MA copolymer, which contains acetate side groups able to self assemble, but is not the case in this study (Fig. 2b, Table 1). Similar results were obtained by the author using alternating copolymers of maleic anhydride with two vinyl ethers: butyl vinyl ether and vinyl methyl triethyleneglycol [30].

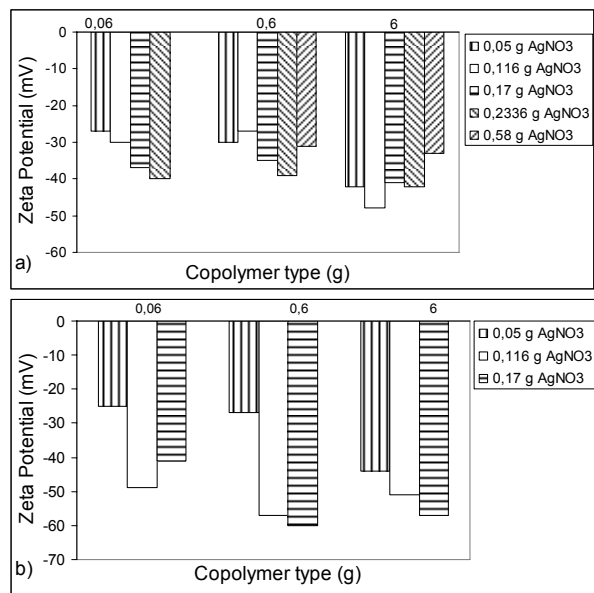


Fig. 4. Zeta potential of  $\text{Ag}^0$  particles synthesized with copolymers ( $\text{StSO}_3$ -MA) (a) and VAc-MA (b)

Surprising is the Zeta potential value which is higher for VAc-MA copolymers comparing with  $\text{StSO}_3$ -MA

copolymers (Fig. 4). This fact can be explained by the weak interaction of VAc-MA copolymer polyelectrolyte with metallic particles. In most of the cases Zeta potential increases with the increase in  $\text{Ag}^0$  concentration, respective the increase of the  $\text{AgNO}_3$ ,  $\text{NaBH}_4$  derivates concentrations. In order to produce more  $\text{Ag}^0$ , the concentrations of the electrolyte from the system was increased, fact which determined the increase of Zeta potential for the metallic particles stabilized with polyelectrolyte. Due to the negative charge of the polymers, Zeta potential increases with the increase of polyelectrolyte concentration.

The UV analyses of  $\text{Ag}^0$  nanoparticles aqueous dispersions are presented in Fig. 5.  $\lambda_{\text{max}}$  obtained from UV spectra of  $\text{StSO}_3$ -MA copolymers (Fig.5a) have similar results with particles average size determined through DLS analyses (Fig.2a). These results are similar with the previously published data [8, 26].

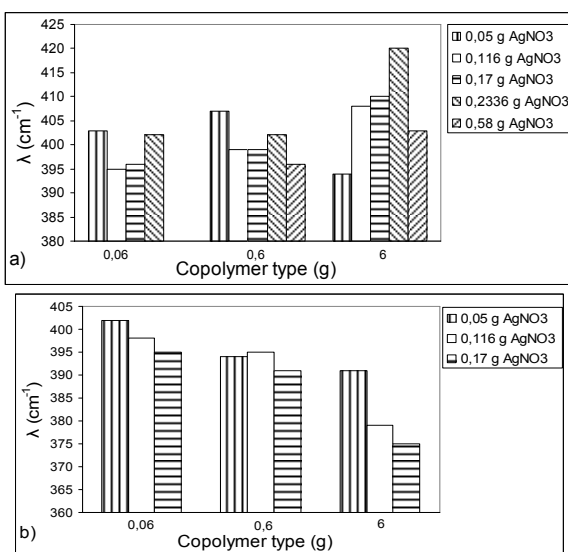


Fig. 5.  $\lambda_{\text{max}}$  from UV spectra of  $\text{StSO}_3$ -MA (a) and VAc-MA (b) copolymers

For VAc-MA copolymers the phenomenon is opposite:  $\lambda_{\text{max}}$  (Fig. 5b) decrease at the same time with the average size of the particles (Fig. 2b), possible due to the different interactions between the  $\text{Ag}^0$  particles surface and the polyelectrolyte based on VAc (Fig. 2b). If particles have larger dimensions, the ratio surface/volume is smaller and the plasmon adsorption changes.

$\lambda_{\text{max}}$  is around 400 nm due to plasmon absorption band, similar with the previously published results [8, 17, 23, 26]. Surface plasmon resonance absorbance is sensitive not only to nature, size, and shape of nanoparticles, but also to the nature of their surrounding media (Fig.5b). These studies allowed us to obtain similar results for other alternating copolymers of maleic anhydride [30].

The IR spectrum of the final product is shown in Fig. 6 and 7 which demonstrates silver encapsulation in  $\text{StSO}_3$ -

MA and VAc-MA copolymers in solid state. The strong absorption at  $3666 \text{ cm}^{-1}$  evidence that the product contains a  $-\text{OH}$  bond from VAc-MA copolymer (Fig. 6), also present at  $1254$  and  $1028 \text{ cm}^{-1}$ , but of weaker intensity. Increasing quantities of silver from the final samples determines the decrease of the peaks intensities, leading to complete disappearance of some peaks at maximum quantity of  $\text{Ag}^0$ . A weak band at  $1699 \text{ cm}^{-1}$  most probably belongs to the  $\text{C}=\text{O}$  bond in macromolecule units. The peaks between  $1550$ - $1620 \text{ cm}^{-1}$  and  $1300$ - $1450 \text{ cm}^{-1}$  characterize  $\text{COO}^-$  bond, but these are absent in the samples with a higher quantity of  $\text{Ag}^0$ , this may indicate silver bonding.

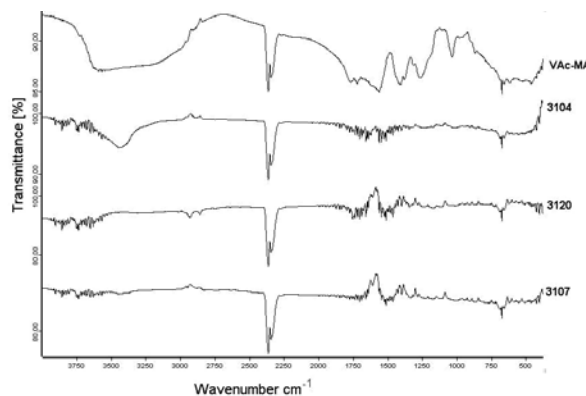


Fig. 6. The FTIR spectra for the VAc-MA copolymer before and after the  $\text{Ag}^0$  different quantities adding

The IR data for  $\text{StSO}_3$ -MA copolymer (Fig. 7) after the  $\text{Ag}^0$  adding present a  $1636 \text{ cm}^{-1}$  peak decreased at lower frequencies. The decrease of  $\text{C}=\text{O}$  adsorption frequency indicates a strong metal-ligand bond formed between the metallic ions and the carboxylic oxygen from the carboxylate salts. The spectra contains absorption bands related to  $\text{O}=\text{S}=\text{O}$  group from  $1418 \text{ cm}^{-1}$  and  $1127 \text{ cm}^{-1}$ .

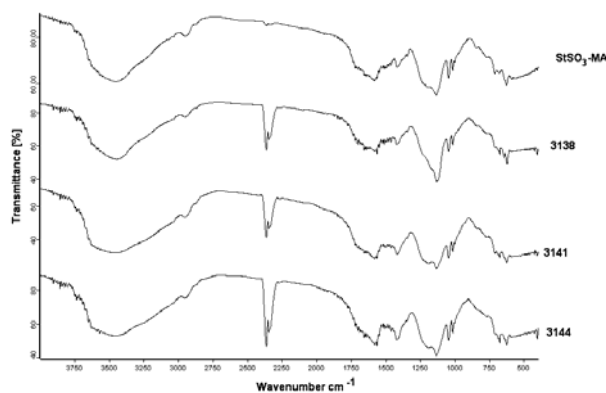


Fig. 7. FTIR spectra of  $\text{StSO}_3$ -MA copolymer before and after different quantities adding (samples from Table 1)

For SEM analyses (Fig. 8, 9) a drop from every sample deposited on a carbon double adhesive band. The samples

were left overnight for water evaporation. Association of the particle after the water evaporation depends on the ratio polymer-silver. The silver particles remain dispersed in polymer matrix for samples 3103 (0.6156g Ag/100 g cop.) and for samples 3104 (6.156g Ag/100 g cop.) silver particles tend to associate, but the particles counter remains although demarcation. Increasing the concentration of the silver generating precursors ( $\text{AgNO}_3$ ) for sample 3121 (123.2g Ag/100 g cop.), comparative with sample 3105, determines the dimensions increase of silver crystalline particles. The counter more or less diffused of Ag particles sustains the fact that these are well dispersed in the copolymer matrix on all three spatial dimensions. Mechanism for crystallite forming may be explained through correlation of properties for moist material, surface tensions, evaporation-driven convective flows and capillary flow, data explained also in the literature (31).

Mixtures with very low concentrations of polyelectrolyte,  $\text{StSO}_3\text{-MA}$  copolymers, have Ag crystalline particles, similarly to case mentioned in Fig.8a, b, c, d. In fig.9a, b SEM images show both composites, which contain copolymers and silver: 3140 (61.56g Ag/100g cop.) and 3143 (123g Ag/100 g cop.). Hybrid 3143 contains a big quantity of Ag and forms crystalline particles of big dimensions, but smaller than copolymer particles Fig. 8.

The decrease of the metal quantity from the samples, for both polyelectrolytes, forms silver crystals with low dimensions. SEM images from Fig. 8, 9 evidence information similarly with others hybrids containing  $\text{Ag}^0$  [4, 31-33].

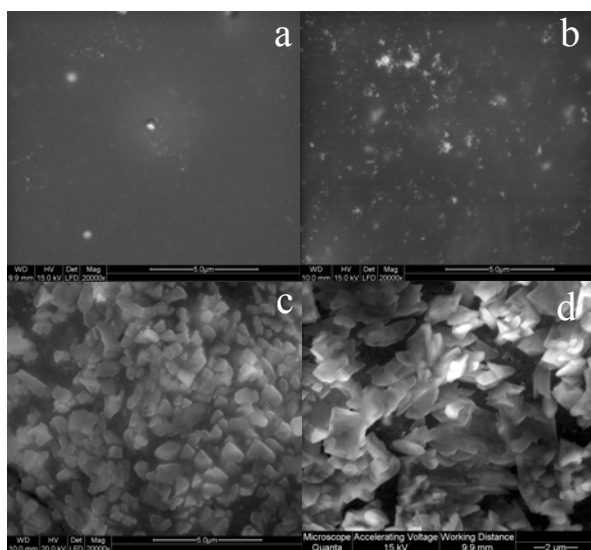


Fig. 8. SEM images of VAc-MA +Ag copolymer hybrids (a – 3103, b -3104, c – 3105, d - 3121) (Synthesis conditions as in Table 1)

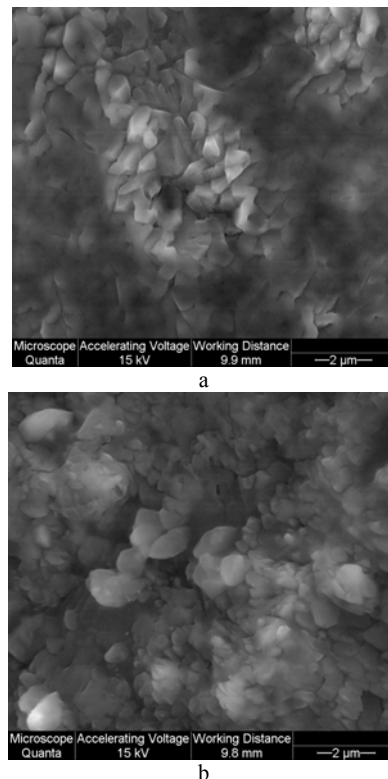


Fig. 9. SEM images for  $\text{StSO}_3\text{-MA} + \text{Ag}$  copolymers a-140, b-3143)(Synthesis conditions as in Table 1)

Information about crystalline state of  $\text{Ag}^0$  particles obtained after hybrids drying can be reached from X-ray diffraction diagrams (Fig. 10). The diffraction maxima ( $38.15^\circ$ ,  $44.4^\circ$ ) corresponding to fcc structures (face centered cubic) [6,12,13,15] are characteristic for  $\text{Ag}^0$  and are absent from the polyelectrolyte diagram. The peak intensity increases with the increase of  $\text{Ag}^0$  concentration from the hybrids (3154, 3153). Side dimensions of the crystal cubes are 22.5 nm for sample 3153 and 14.1 nm for sample 3154.

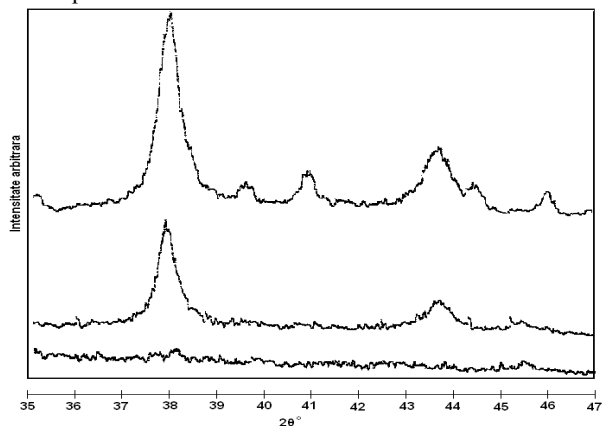


Fig. 10. XRD for hybrids  $\text{Ag}^0 - \text{StSO}_3 - \text{MA}$  (sample 3154, 3153, copolymer  $\text{StSO}_3 - \text{MA}$  – see Table 1)

Dried samples used for characterization can be redispersed in water under stirring. In these samples, as well as in the aqueous dispersions, of  $\text{Ag}^0$  particles in polyelectrolytes solutions, is evidenced by X-ray fluorescence diagrams presence of metallic nanoparticles (Fig.11).

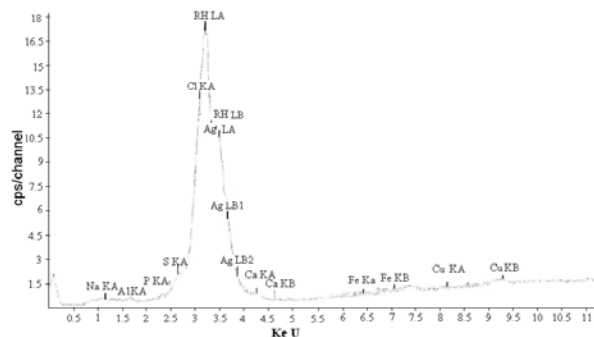


Fig. 11. The X-ray fluorescence spectra for the aqueous solution of the 3154 hybrid system obtained after the synthesis (see Table1).

Results from Fig.11 are similar with the ones published by other authors [16, 32, 34-36]. The diagrams confirm the presence of  $\text{Ag}^0$  nanoparticles, synthesized through  $\text{AgNO}_3$  reduction with  $\text{NaBH}_4$  in aqueous solutions, and characterized in Fig. 2-5.

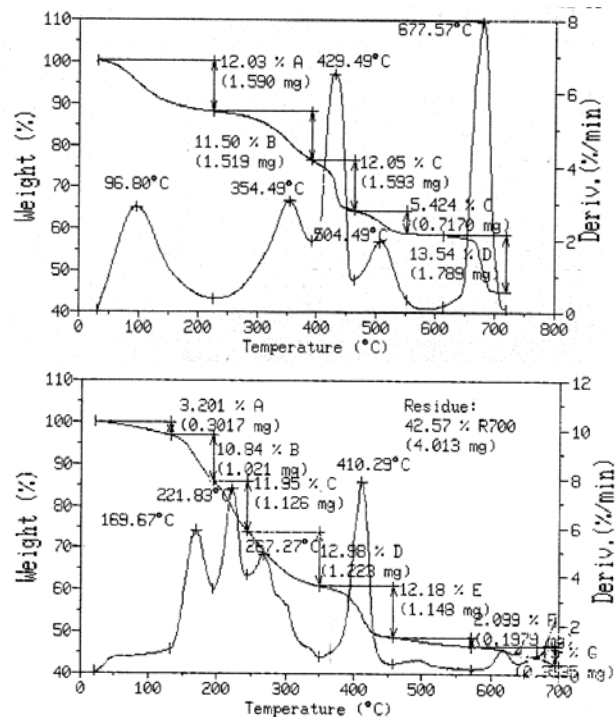


Fig. 12. TGA and DTG curves for the  $\text{StSO}_3$ -MA (a) and VAc-MA (b) copolymers

For thermal decomposition of the polymers, the nature of the macromolecular chains substitutes is the controlling factor (37-38). The carboxyl groups from the alternating copolymers of maleic anhydride decrease the thermal stability (30). The thermal stability increases in the metallic nanoparticles presence in some cases, for silver composites (39, 40).

Using these information we considered useful to observe the thermal stability modification of the synthesized hybrids.

TGA and DTG curves are presented for copolymers with MA and styrene sulphonate in Fig.12a and for vinyl acetate in Fig. 12b.

Similarly with previous published data (38) there are some thermal decomposition stages, which depend on the nature of maleic anhydride comonomers.

In the domain of temperature between 20-150°C are registered weight losses due to the adsorbed water. For the copolymers with hydrophilic comonomer (styrene sulphonate), the quantity of water lost in this domain of temperature is higher (Fig.10 a) than for the vinyl acetate comonomer (Fig10 b).

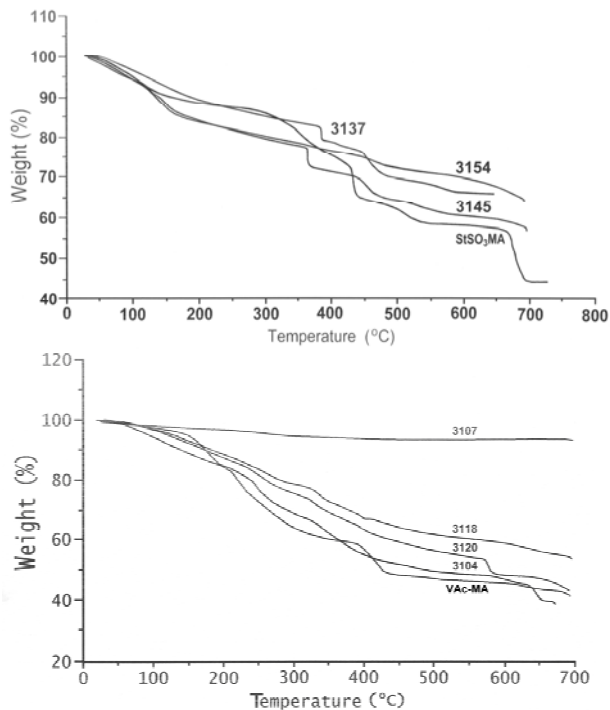


Fig. 13. The TGA curves for the  $\text{StSO}_3$ -MA (a), VAc-MA (b) copolymers (synthesis conditions as in Table 1)

While temperature increases, many stages of decomposition appear due to the loss of monomer substituents [37, 38]. For  $\text{StSO}_3$ -MA copolymer, two domains of temperature in the range 250-450°C were observed (Fig. 10 a), as for the other copolymer three stages of important losses were observed between 150-350°C (Fig. 10 b). The thermal degradation of the main monomer chain from the  $\text{StSO}_3$ -MA copolymer

takes place in the of temperature domain 450-550°C (Fig. 10 a) and for VAc-MA copolymer takes place between 350-450°C (Fig.10 b). Comparative analysis of the data from Fig.10 indicates the fact that the thermal degradation begins at lower temperature for the VAc-MA copolymer than for StSO<sub>3</sub>-MA copolymer (Fig.10 b). In the presence of Ag<sup>0</sup> nanoparticles, thermal decomposition begins at higher temperatures simultaneously with the increase of organic component concentration (Fig. 13).

The composites obtained with StSO<sub>3</sub>-MA (Fig. 12 a) show the same characteristic of thermal stability in comparison with the VAc-MA copolymer (Fig. 12 b).

#### 4. Conclusions

In conclusion the polyelectrolyte like StSO<sub>3</sub>, MA, VAc-MA presence allows to get Ag<sup>0</sup> nanodispersions in the aqueous medium. The StSO<sub>3</sub>-MA copolymers ensure the time stability for Ag<sup>0</sup> nanoparticles dispersion at high concentration. The mean diameters of the stabilized particles are smaller than for the other copolymer. The UV, fluorescence and X-ray studies confirms the nanoparticle existence.

The SEM images and the X-ray analyzes evidence the particle incorporation in the polymeric matrix. These are crystalline nanoparticles which at low concentrations of polyelectrolyte are strongly aggregated in solid phase.

#### Acknowledgments

The authors gratefully acknowledge the financial support of this research by the POSDRU/89/1.5/S/54785 research project.

#### References

- [1] L. Nicolais, G. Carotenuto Eds. "Metal-Polymer Nanocomposites", Wiley Int. Publ., 2005
- [2] J. H. Yeum, Q. Sun, Y. Deng, *Macromolecular Mat. and Eng.* **290**, 58 (2005).
- [3] C. J. Huang, F. S. Shieu, *Coll.Polymer Sci.* **284**, 192 (2005).
- [4] B. Yin, H. Ma, S. Wang, S. Chen, *J. Phys. Chem. B* **107**, 8898 (2003).
- [5] D. Radziuk, D. G. Shchukin, A. Skirtach, H. Mohwald, G. Sukhomkov, *Langmuir* **23**, 4612 (2007).
- [6] R. Gunawidjaja, C. Jiang, S. Peleshanko, M. Ornatska, S. Singamaneni, V. Tsukruk, *Adv. Funct. Mater.* **16** 2024 (2006).
- [7] Y. F. Huang, Y. W. Lin, H. T. Chang, *Langmuir* **23**, 12777 (2007).
- [8] I. Sondi, D. V. Goia, E. Matijevic, *J. Coll. Int. Sci.*, **260**, 75 (2003).
- [9] I. Hussain, M. Burst, A. J. Papsworth, A. I. Cooper, *Langmuir*, **19**, 4831 (2003).
- [10] H. Bonneman, S. S. Botha, B. Blagergroen, U. M. Linkov, *Appl. Organometal. Chem.* **19**, 768 (2005)
- [11] Z. Shen, H. Duan, H. Frey, *Adv. Mater.* **19**, 349 (2007).
- [12] Y. M. Mohan, K. Lee, T. Premkumar, K. E. Geckeler *Polymer* **48**, 158 (2007)
- [13] V. Thomas, M. M. Yallapu, S. Sreedhar, S. K. Bajjdi, *J. Coll. Int. Sci.*, **315**, 389 (2007).
- [14] J. Zhang, S. Xu, E. Kumaceva, *Adv. Mater.* **17**, 2336 (2005)
- [15] D. Zhang, L. Qi, J. Yang, J. Ma, H. Cheng, L. Huang, *Chem. Mater.*, **16**, 872 (2004).
- [16] Y. Shiraishi, M. Toshima, *Coll and Surf. A: Physicochem. Eng. Aspects*, **169**, 59 (2000).
- [17] B. Ersov, A. Henglein, *J. Phys. Chem. B* **102**, 10663S (1998).
- [18] R. Sardar, J. W. Park, J. S. Shumaker-Parry, *Langmuir*, **23**, 11883 (2007).
- [19] S. Liu, J. Yue, A. Gedanken, *Adv. Mater.* **13**, 656 (2001).
- [20] L. M. Bronstein in ref. 1 p. 123.
- [21] A. Laschewsky, *Adv. in Polym. Sci.*, **124**, 25 (1995), Springer Verlag, Berlin, Heidelberg, N.Y
- [22] D. Donescu, S. Serban, C. Petcu, *Mat. Plastice* **38** 133 (2001).
- [23] A. Heilman in ref (1) p.183
- [24] H. Bao, G. Chumanov, R. Czerw, D. L. Caroll, St. H. Foulger, *Coll. Polym. Sci.* **283**, 653 (2005)
- [25] C. Hen, L. Wang, G. Jiang, H. Yu, *Rev. Adv. Mater. Sci.*, **11**, 1 (2006).
- [26] J. R. Morones, W. Frey, *Langmuir*, **23**, 8180 (2007).
- [27] J. Dong, D. R. Witcomb, A. V. Mc Cormick, H. T. Davis, *Langmuir*, **23**, 7963 (2007)
- [28] C. Petit, P. Lixon, M. P. Pileni, *J. Phys. Chem.* **97**, 12974 (1993).
- [29] K. T. Wang., I. Illopoulos, R. Audebert, *Polym. Bull.* **20**, 577 (1988).
- [30] D. Donescu et al. in press
- [31] A. Kamyshny, M. Ben-Moshe, S. Aviezer, S. Magdassi, *Macromol. Rapid Comm.* **26**, 281 (2005).
- [32] Z. Zhang, L. Zhang, S. Wang, W. Chen, Y. Lei, *Polymer* **42**, 8315 (2001).
- [33] L. Wang, D. Chen, *Coll. Polym. Sci.* **284**, 449 (2006).
- [34] S. Shanmugam, B. Viswanathan, T. K. Varadarajan, *Mat. Chem. Phys.* **95**, 51 (2006).
- [35] A. Gautam, P. Tripathy, S. Ram, *J. Mater. Sci.*, **41**, 3007 (2006).
- [36] H. S. Shim, H. C. Choi, Y. Jung, S. B. Kim, H. J. Song, H. J. Shin, *Chem. Phys. Letters*, **383**, 418 (2004).
- [37] K. Kamius, M. Swiatek *J. Thermal Anal.* **46**, 1383 (1996).
- [38] T. Barnah, M. L. Laskar, *J. Appl. Polym. Sci.* **60**, 649 (1996).
- [39] S. Quingwen, L. Yi, X. Jianwei, J. Y. Hu, M. Yuen, *Polymer* **48**, 3317 (2007).
- [40] P. S. K. Murthy, Y. Mohan, K. Varaprasad, B. Sreedhar, K. M. Raju, *J. Coll. Int. Sci.* **318**, 217 (2008).

\*Corresponding author: ralucaomoghi@yahoo.com